Original Article

Effects of ginsenoside compound K on colitis-associated colorectal cancer and gut microbiota profiles in mice

Li Shao[1], Yin-Ping Guo[2,3,4], Li Wang[2,3], Man-Yun Chen[2,3], Wei Zhang[2,3], Sheng Deng[5], Wei-Hua Huang[2,3,6]

[1]Department of Pharmacognosy, School of Pharmacy, Hunan University of Chinese Medicine, Changsha, China; [2]Department of Clinical Pharmacology, Xiangya Hospital, Central South University, Changsha, China; [3]National Clinical Research Center for Geriatric Disorders, Xiangya Hospital, Central South University, Changsha, China; [4]Institute of Clinical Medicine, the First Affiliated Hospital of University of South China, Hengyang, China; [5]Department of Pharmacy, Xiangya Hospital, Central South University, Changsha, China; [6]NHC Key Laboratory of Birth Defect for Research and Prevention (Hunan Provincial Maternal and Child Health Care Hospital), Changsha, China

Contributions: (I) Conception and design: WH Huang; (II) Administrative support: S Deng; (III) Provision of study materials or patients: W Zhang; (IV) Collection and assembly of data: L Shao, YP Guo; (V) Data analysis and interpretation: L Shao, YP Guo, L Wang, MY Chen; (VI) Manuscript writing: All authors; (VII) Final approval of manuscript: All authors.

Correspondence to: Wei-Hua Huang. Department of Clinical Pharmacology, Xiangya Hospital, Central South University, Changsha, China. Email: endeavor34852@csu.edu.cn; Sheng Deng. Department of Pharmacy, Xiangya Hospital, Central South University, Changsha, China. Email: dengsxy@sina.com.

Background: Ginsenoside compound K (GC-K), generated from ginseng saponins bioconverted by gut microbiota, has potential anti-colorectal cancer (CRC) effects. Meanwhile, GC-K may interact with gut microbiota, playing important roles in the occurrence and development of CRC. However, the effects of gut microbiota on the preventive and therapeutic effects of GC-K in CRC remain to be elucidated.

Methods: The anti-CRC effects of GC-K were evaluated in an azoxymethane/dextran sulfate sodium (AOM/DSS)-induced colitis-associated CRC Balb/c mice model under the dosage of 30 and 60 mg/kg. Stool samples were collected during the experiments for profiling gut microbiota by *16S rRNA* sequencing. Correlative analysis between gut microbiota and anti-CRC effect of GC-K was also assessed. Finally, the anti-CRC effect of *Akkermansia muciniphila* (*A. muciniphila*) was validated in CRC cell lines.

Results: GC-K could significantly suppress tumor growth *in vivo* at the dosage of 60 mg/kg without exogenous interference of gut microbiota. Moreover, dysbiosis of gut microbiota was observed in the CRC model group, which could be recovered by GC-K treatment. In particular, *A. muciniphila*, which could inhibit the proliferation of HCT-116, HT-29, and LOVO cells, was significantly up-regulated by GC-K.

Conclusions: GC-K was verified to suppress the tumor growth of AOM/DSS-induced colitis-associated CRC through the modulation of gut microbiota, partially by up-regulation of *A. muciniphila*.

Keywords: Ginsenoside compound K (GC-K); colorectal cancer (CRC); gut microbiota; *Akkermansia muciniphila* (*A. muciniphila*); *16S rRNA* gene sequencing

Submitted Jan 12, 2022. Accepted for publication Mar 10, 2022.
doi: 10.21037/atm-22-793
View this article at: https://dx.doi.org/10.21037/atm-22-793

Introduction

Colorectal cancer (CRC) is one of the most common cancers worldwide, with high incidence and mortality in 2020. However, the molecular mechanisms of the occurrence and progression of CRC are not yet fully understood (1). A risk factor for the occurrence of CRC is ulcerative colitis (UC), which was reported that the risk for occurrence of CRC is up to 30% for 35 years of UC patients (2). Meanwhile, UC is often accompanied by gut

© Annals of Translational Medicine. All rights reserved.

microbiota dysbiosis and chronic inflammation (2). Gut microbiota are a complex community in the gastrointestinal tract and can be influenced by many factors, such as drugs and disease (3). Accumulating evidence indicates that gut microbiota are significantly associated with the occurrence and development of CRC (4,5). For example, gut microbiota could influence the inflammation process through affecting generation of short-chain fatty acids in the aspect of metabolome (4), and also play crucial roles in the development and function of the immune system (6-8). Therefore, targeting the gut microbiota may be a new strategy for CRC therapy (9).

Ginsenoside compound K (GC-K) belongs to Dammarane-type tetracyclic triterpenoids, and is one of the main metabolites of ginseng saponins *in vivo* and is bioconverted by gut microbiota (10-12). It has been shown various pharmacological activities, such as anti-diabetic, anti-aging, anti-allergic, anti-inflammation and anti-tumor effects, in which the anti-CRC effect attracts increasing focus (13,14). However, the pertinent mechanisms are not well known. In previous studies, although GC-K could inhibit the proliferation and promote the apoptosis of HCT-116 and HT-29 cells, as well as the growth of xenograft tumors (15-17), the effects of GC-K on CRC *in situ* are still unverified. Meanwhile, the anti-CRC mechanism of GC-K is also not yet fully clarified.

As the absolute oral bioavailability of GC-K is about 35% (18), GC-K could be metabolized to yield protopanaxadiol only by β-glycosidase secreted by gut microbiota *in vivo* (19,20), which implies that GC-K could be delivered into the gastrointestinal tract to interplay with gut microbiota after oral administration. In addition, our previous study found that ginseng saponins could prevent colitis-associated CRC partially via modulating gut microbiota profiles (21,22). Accordingly, we hypothesized that GC-K could inhibit the growth of CRC *in situ* via benefiting from gut microbiota.

In this study, a Balb/c mouse model was induced and constructed by azoxymethane (AOM)/dextran sulfate sodium (DSS), which led to the death of epithelial cells, resulting in acute and chronic intestinal inflammation. GC-K was orally administered to evaluate the anti-CRC effect *in vivo*. The disease activity index (DAI) scores, colon length and tissue evaluation, tumor number and size, and histological assessment were employed to assess the attenuation effect of GC-K on colitis-associated CRC development. Furthermore, *16S rRNA* sequencing was used to analyze gut microbiota profiles. The results showed that the relative pathological indexes were significantly decreased in the GC-K high-dose group compared with the model group. Dysbiosis of gut microbiota was observed in the AOM/DSS-induced model group, which could be partially recovered by GC-K treatment. Importantly, the up-regulated gut microbe *Akkermansia muciniphila* (*A. muciniphila*) could significantly inhibit the proliferation of HCT-116, HT-29, and LOVO cells. Therefore, due to the regulation of GC-K on gut microbiota, GC-K exerted potential anti-CRC effects partially by benefiting from gut microbiota. We present the following article in accordance with the ARRIVE reporting checklist (available at https://atm.amegroups.com/article/view/10.21037/atm-22-793/rc).

Methods

Chemicals and reagents

GC-K was provided by Chengdu Push Bio-technology Co., Ltd. (Sichuan, China). AOM was purchased from Sigma Co., Ltd. (MO, USA), and DSS with molecular weight at 36–50 kDa was obtained from MP Biomedicals LLC (CA, USA). The Standard AIN-93G chow was manufactured by Trophic Feed High-tech Co., Ltd. (Jiangsu, China).

The bacteria genomic DNA extraction kit was supplied by Qiagen Co., Ltd. (Hilden, Germany). The mixture PCR product purification kit was provided by Axygen Biosciences Co., Ltd. (CA, USA). The sequencing library generation kit was bought from Illumina Co., Ltd. (CA, USA).

Animals and experimental design

Balb/c mice (male, 6 weeks, 18±2 g), supplied by Hunan SJA Laboratory Animal Co., Ltd. (Hunan, China) with a license No. 43004700051266, were acclimated to specific-pathogen-free (SPF) conditions at 22±2 ℃ and 60%±5% humidity with a 12/12-hour light-dark cycle for a week. The animal experimental protocol was approved by the Ethics Committee of Animal Experiments of Central South University (No. 201803070). Experiments were performed in compliance with the "Regulations on the Administration of Laboratory Animals" formulated by the National Science and Technology Commission of the People's Republic of China for the care and use of animals. A protocol was prepared before the study without registration.

Mice were randomly divided into the control group, AOM/DSS model group, low-dose group (30 mg/kg), and high-dose group (60 mg/kg) (n=6, each group). The daily chow consumption of each group was recorded every

© Annals of Translational Medicine. All rights reserved.

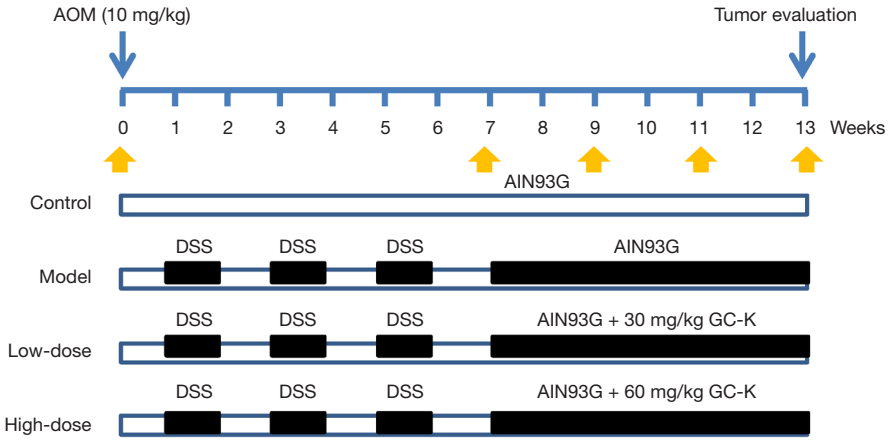

Figure 1 The animal experimental protocol. AOM, azoxymethane; DSS, dextran sulfate sodium; GC-K, ginsenoside compound K.

2–3 days to calculate the average dosage of GC-K in the low/high-dose groups. Except for the control group, the other groups were intraperitoneally injected with AOM (10 mg/kg). After 1 week, mice were freely fed with drinking water with 2.5% DSS for 1 week, followed by pure water for another 1 week (3 cycles). Then, the low-dose and high-dose groups were fed with standard AIN-93G chow containing 220 or 440 ppm of GC-K for 45 days according to previous study (23), and the actual dosage was calculated by the mean body weight and the mean daily chow consumption. The mice were euthanized by cervical dislocation for tumor evaluation, and the colon segments were collected for pathological analysis. The stool samples for *16S rRNA* sequencing analysis were collected at week 0, after AOM/DSS-induction (week 7), at 2 weeks after treatment of GC-K (week 9), at 4 weeks (week 11), and at the last week (week 13) (*Figure 1*). Authors were aware of the group allocation all around the experiments.

DAI and histological assessment

The DAI integrated with the scores of weight loss, stool consistency, and rectal bleeding was used for assessing the intestinal inflammation induced by AOM/DSS during modeling (24). The distal colorectal segments were fixed in 4% paraformaldehyde for hematoxylin and eosin (H&E) staining to evaluate intestinal damage histopathologically.

16S rRNA gene sequencing

Microbial genomic DNA was extracted using the Qiagen QIAamp DNA Stool Mini Kit following the manufacturer's instructions (Qiagen, Germany). The V3-V4 region of the bacterial *16S rRNA* gene was amplified by PCR with bacterial primers 338F 5'- ACTCCTACGGGAGGCAGCAG-3' and 806R 5'-GGACTACHVGGGTWTCTAAT-3'. Then, amplicons were extracted and purified by the AxyPrep DNA Gel Extraction Kit (Axygen Biosciences, CA, USA) and quantified by QuantiFluor™-ST (Promega, WI, USA). The purified amplicons were paired-end sequenced on an Illumina MiSeq platform.

Cell lines and culture

Human CRC cell lines (HCT-116, LOVO, and HT-29 cells) were purchased from Cell Center of Central South University. HCT-116, LOVO, and HT-29 cells were cultured in RPMI 1640, Ham's F-12K, and McCoy's 5A medium supplemented with 10% fetal bovine serum (FBS), respectively. The 3 cell lines were incubated in a humidified atmosphere of 5% CO_2 at 37 ℃. The medium was changed every 1 or 2 days. Cells were trypsinized, harvested, and seeded into a new tissue culture flask when they reached approximately 80% confluence.

A. muciniphila and CRC cell co-culture

CRC cells were seeded in a 24-well plate (5×10^3 cells/well) in medium supplemented with 10% FBS for 24 hours. *A. muciniphila* at logarithmic growth stage were infected at the plural numbers of 100:1 and 1,000:1 to prepare the infectious working fluid, and the microbes were suspended in pure medium without FBS. Cells were exposed to the suspended infectious working fluid for 4 hours, and then

© Annals of Translational Medicine. All rights reserved.

the medium containing *A. muciniphila* was replaced with medium supplemented with 10% FBS. The co-culture was performed for 20 hours with 3 cycles. The medium was discarded, followed by adding trypsin, and then the cells were suspended and counted with a cell counting plate.

Bioinformatics analysis

Raw data were demultiplexed and filtered using QIIME (version 1.9.1), while chimeric sequences were identified and removed by UCHIME. Then, operational taxonomic units (OTUs) were clustered with 97% similarity cutoff using UPARSE (version 7.1 https://drive5.com/uparse/). The taxonomy of each *16S rRNA* gene sequence was analyzed by RDP Classifier (https://rdp.cme.msu.edu/) against the Silva (SSU123) *16S rRNA* database. QIIME was used to calculate alpha and beta diversity of gut microbiota.

Statistical analysis

One-way analysis of variance (ANOVA) with the least significant difference (LSD) post hoc test was applied for statistical analysis in SPSS Statistics software (version 17.0) and GraphPad Prism software (version 7.00), and significant differences were expressed as *P<0.05 and **P<0.01.

Results

GC-K suppressed AOM/DSS-induced colitis-associated CRC

During modeling, mice in the model group showed a distinct loss of weight and appetite, along with diarrhea and rectal bleeding accompanied by AOM/DSS administration. Compared with the control group, the DAI of mice in the model group was significantly increased (*Figure 2A*). The average daily consumption of GC-K in the control, AOM/DSS model, low-dose, and high-dose groups were 2.93±0.25, 3.31±0.39, 3.26±0.40, and 3.25±0.33 g, respectively (*Figure 2B*). Due to the calculation, the actual dosages of GC-K in the low-dose and high-dose groups were 26.99 and 58.65 mg/kg, respectively.

Compared with the control group, the colon length of the model group was significantly shortened, which could be alleviated by GC-K treatment (*Figure 2C,2D*). The tumor size was calculated as described previously (25). Compared with the AOM/DSS model group, the mean tumor size in the high-dose group was significantly decreased, while there was no significant difference in the low-dose group (*Figure 2E,2F*).

H&E staining histological evaluation was used to assess colorectal damage, which was observed according to epithelial cell nuclei, stained nuclei, and disordered structure. H&E staining showed that crypts were aberrant with disordered arrangement, while inflammatory cells infiltrated the submucosa in the model group to obviously induce abnormal colon tissue characteristics. However, the pathological symptoms could be relieved by GC-K treatment (*Figure 2G*). Consequently, our data indicated that GC-K suppressed AOM/DSS-induced colitis-associated CRC.

Diversity and taxonomic differences of gut microbiota

The Simpson index (diversity index) and Chao1 (richness estimation index) were employed to characterize gut microbial alpha diversity (*Figure 3A,3B*). Chao1 indicated that gut microbial species richness gradually decreased in the model group. However, the microbial species richness of the GC-K groups was partially restored. The Simpson index increased at subsequent testing weeks compared with week 0. For alpha diversity, reduced microbial species and abundances of dominant microbes indicated that gut microbiota were disordered in the model group. Compared with the model group, the alpha diversity and coverage index significantly increased in the high-dose group at week 13. The data showed that GC-K could increase the alpha diversity of gut microbiota in the AOM/DSS induced colitis-associated CRC model.

The results of beta diversity showed that all of the samples were clustered with an equal starting point at week 0 (Figure S1A), and classified into 2 groups after AOM/DSS intervention at week 7 (Figure S1B). Subsequently, gut microbiota in the GC-K groups gradually became distinguished from the model group (Figure S1C,S1D and *Figure 3B*). These results implied that the beta diversity of gut microbiota could be remodulated by GC-K in colitis-associated CRC mice.

Taxonomical classification was performed at the phylum and genus levels. At the phylum level (*Figure 3C*), compared with the control group, *Firmicutes* and *Verrucomicrobia* gradually decreased, while *Bacteroidetes* increased in the AOM/DSS-induced colitis-associated CRC model. *Verrucomicrobia* could be recovered by GC-K treatment. At the genus level (Figure S2A-S2D), *Uncultured_Bacteroidales_bacterium* and *Rikenellaceae* were enriched in the model group, but *Akkermansia*, *Bifidobacterium*, and *Staphylococcus*

© Annals of Translational Medicine. All rights reserved.

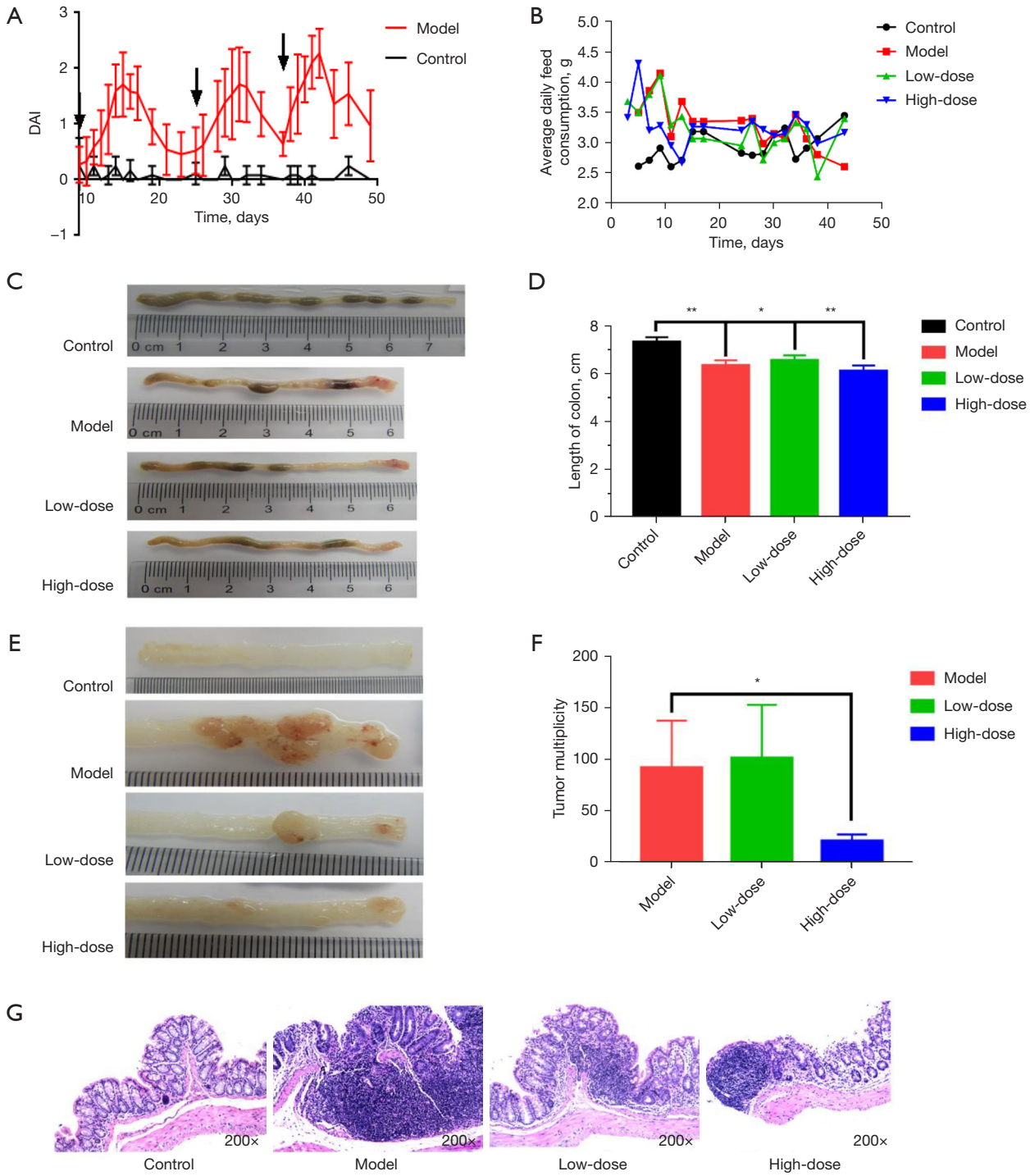

Figure 2 GC-K suppressed AOM/DSS-induced CRC. (A) DAI during modeling. The black arrows indicated the DAI scores of normal mice; (B) average daily chow consumption of each group; (C) typical colorectal macroscopic morphology; (D) colorectal length; (E) typical macroscopic morphology of a colorectal tumor; (F) colorectal tumor size; (G) representative HE staining images in each group. *, P<0.05; **, P<0.01. (n=6). DAI, disease activity index; GC-K, ginsenoside compound K; AOM, azoxymethane; DSS, dextran sulfate sodium.

© Annals of Translational Medicine. All rights reserved.

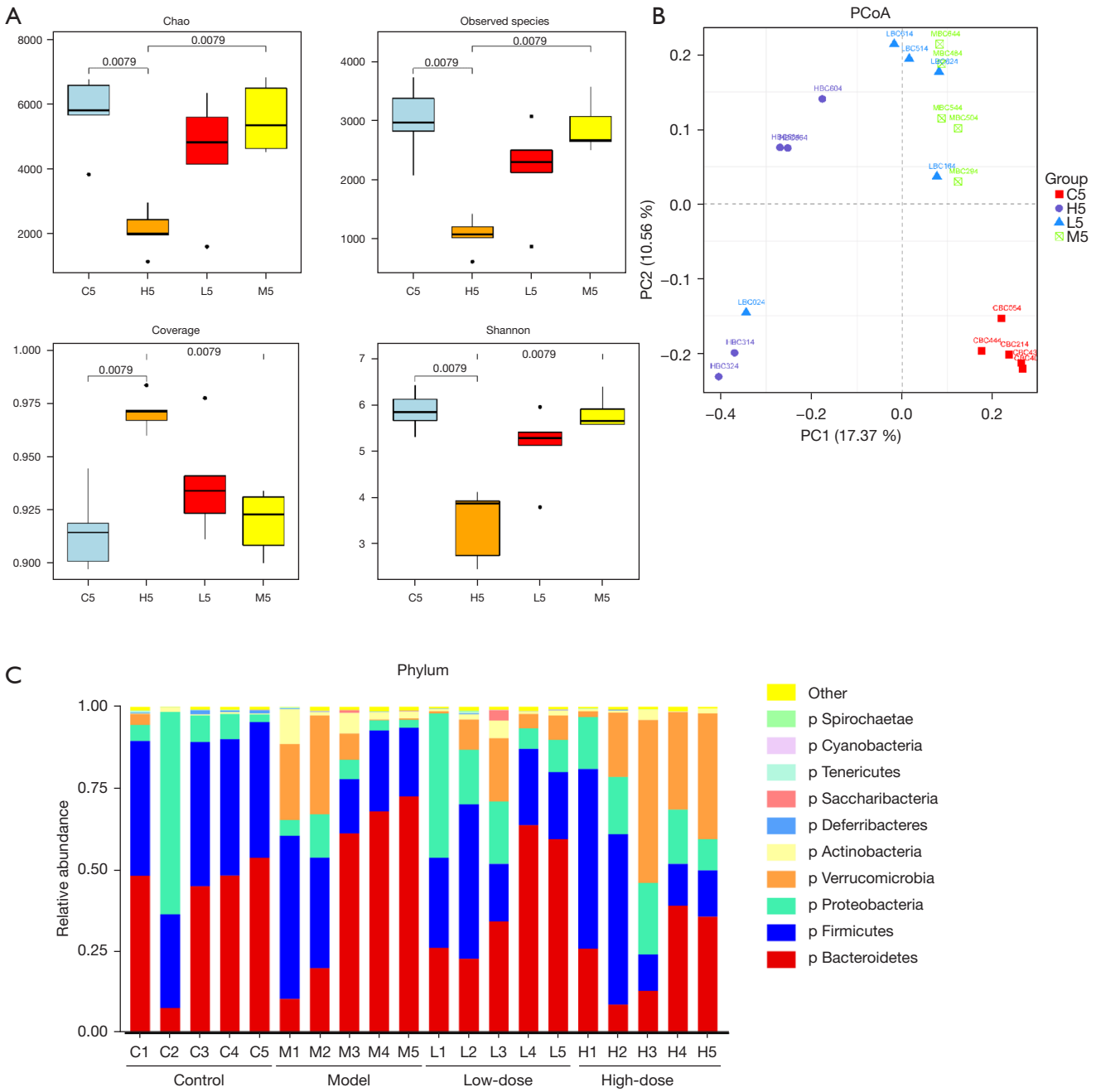

Figure 3 Gut microbiota profile alteration induced by GC-K. (A) Alpha diversity at 13 weeks; (B) beta diversity at 13 weeks; (C) bacterial annotation at the phylum level. The labels of X axis consist of capital letters and Arabic numerals. C, M, L, and H mean control, model, low-dose, and high-dose group, respectively; 1, 2, 3, 4, and 5 indicate time points at 0, 7, 9, 11, and 13 weeks, respectively (n=5). PCoA, principal coordinates analysis; GC-K, ginsenoside compound K.

were relatively decreased after AOM/DSS intervention in the model group. Meanwhile, *Akkermansia* and *Lachnoclostridium* were increased in the high-dose group, which indicated that they could be up-regulated by GC-K.

Biomarker discovery and correlation analysis of gut microbiota

Linear discriminant analysis effect size (LEfSe) analysis

© Annals of Translational Medicine. All rights reserved.

was used to discover differentially abundant taxon. Seven gut microbes were found and mainly categorized into Bacteroidetes, Firmicutes, and *Verrucomicrobia* [P<0.05, linear discriminant analysis (LDA) scores >4, *Figure 4A,4B*]. *Alistipes*, *Oscillibacter*, and *Ruminiclostridium_9* were significantly increased in the control group, while *Rikenellaceae_RC9_gut_group* was enriched in the model group and could be a potential biomarker for AOM/DSS-induced CRC (*Figure 4C*). *Akkermansia spp*. and *Lachnoclostridium spp*. were significantly enriched in the high-dose group, which demonstrated that GC-K could up-regulate their abundance (*Figure 4D,4E*).

The relationship between tumor size and differentially abundant taxon was evaluated by Spearman's correlation index. The relative abundance of *Akkermansia spp*. was inversely correlated with tumor size, while *Rikenellaceae_RC9_gut_group* showed a positive association. Therefore, GC-K might enhance anti-CRC effects pertinent to up-regulating *Akkermansia*.

Akkermansia suppressed CRC cell proliferation in vitro

To further investigate the tumor-inhibiting ability of *Akkermansia spp*., the effects of *Akkermansia spp*. on CRC cell proliferation were examined *in vitro*. The results showed that *Akkermansia spp*. significantly inhibited proliferation in HCT-116 (P<0.01), HT-29 (P<0.05), and LOVO (P<0.01) cells compared with the corresponding control cells (*Figure 5*).

Discussion

As the main active metabolite of ginseng saponins, GC-K was reported to have anti-CRC effects. In current stage, the anti-CRC mechanisms of GC-K involved in activating CAMK-IV/AMPK pathways refers to apoptosis, increasing Ca^{2+} influx for cell death (15-17,26). However, most studies have focused on the effects of GC-K using a xenograft model in nude mice, as well as *in vitro* studies (17,26). Thus, it is necessary to evaluate the effects of GC-K on CRC *in situ*.

Colitis-associated CRC was induced by AOM and DSS (23,27). According to the dosage of GC-K used in animals and human beings (19,28,29), GC-K was set at 30 and 60 mg/kg to avoid adverse events, and their actual dosage was consistent with the design. After 6 weeks of GC-K intervention, the results of tumor size showed that 60 mg/kg GC-K could significantly suppress the growth of colitis-associated CRC. However, no obvious effects were observed in the low-dose group, which might be due to the unsaturation of carrier-mediated hepatic uptake and esterification of GC-K (18).

The results of taxonomy annotation and LEfSe analysis showed that *Akkermansia spp*. could be down-regulated and *Rikenellaceae_RC9_gut_group* could be up-regulated by colitis-associated CRC, the effects of which could be reversed by GC-K. Moreover, *Lachnoclostridium* could be up-regulated by GC-K. These data suggested that *Rikenellaceae_RC9_gut_group* might be a biomarker of CRC, while *Akkermansia spp*. might play an important role in the anti-CRC effects of GC-K.

Rikenellaceae_RC9_gut_group belongs to *Bacteroidetes*, which was shown to increase in an isoproterenol-induced acute myocardial ischemia model, leading to intestinal permeability and impaired intestinal barrier and gut inflammation (30). Meanwhile, *Rikenellaceae* is associated with lipid metabolism (31). However, the relationship between *Rikenellaceae* and CRC is not well understood. *Akkermansia spp*., a human intestinal mucin-degrading bacterium, contains only 1 species, *A. muciniphila* (32,33). The abundance of *A. muciniphila* was shown to decrease in a DSS-induced chronic colitis mice model, while anti-inflammatory effects and improved clinical parameters were observed after intervention of *A. muciniphila* (34,35). Additionally, *A. muciniphila* is significantly reduced in inflammatory bowel disease patients, and mice with this condition could secrete a purified membrane protein, Amuc_1100, to modulate $CD8^+$ T cells (36).

Moreover, we also indicated that the gut microbe *A. muciniphila* showed anti-proliferative effects on CRC cells *in vitro*. Other gut microbes, such as *Rikenellaceae spp*., need further study to investigate their anti-CRC effects *in vitro* and *in vivo*. Additionally, the regulation of the host immune response and remodulation of the tumor microenvironment by gut microbes should also be further investigated in the context of anti-CRC effects.

Conclusions

GC-K was firstly verified to suppress the growth of AOM/DSS-induced colitis-associated CRC *in vivo*. The abundance of *A. muciniphila* was decreased by colitis-associated CRC, which could be restored by GC-K and may

© Annals of Translational Medicine. All rights reserved.

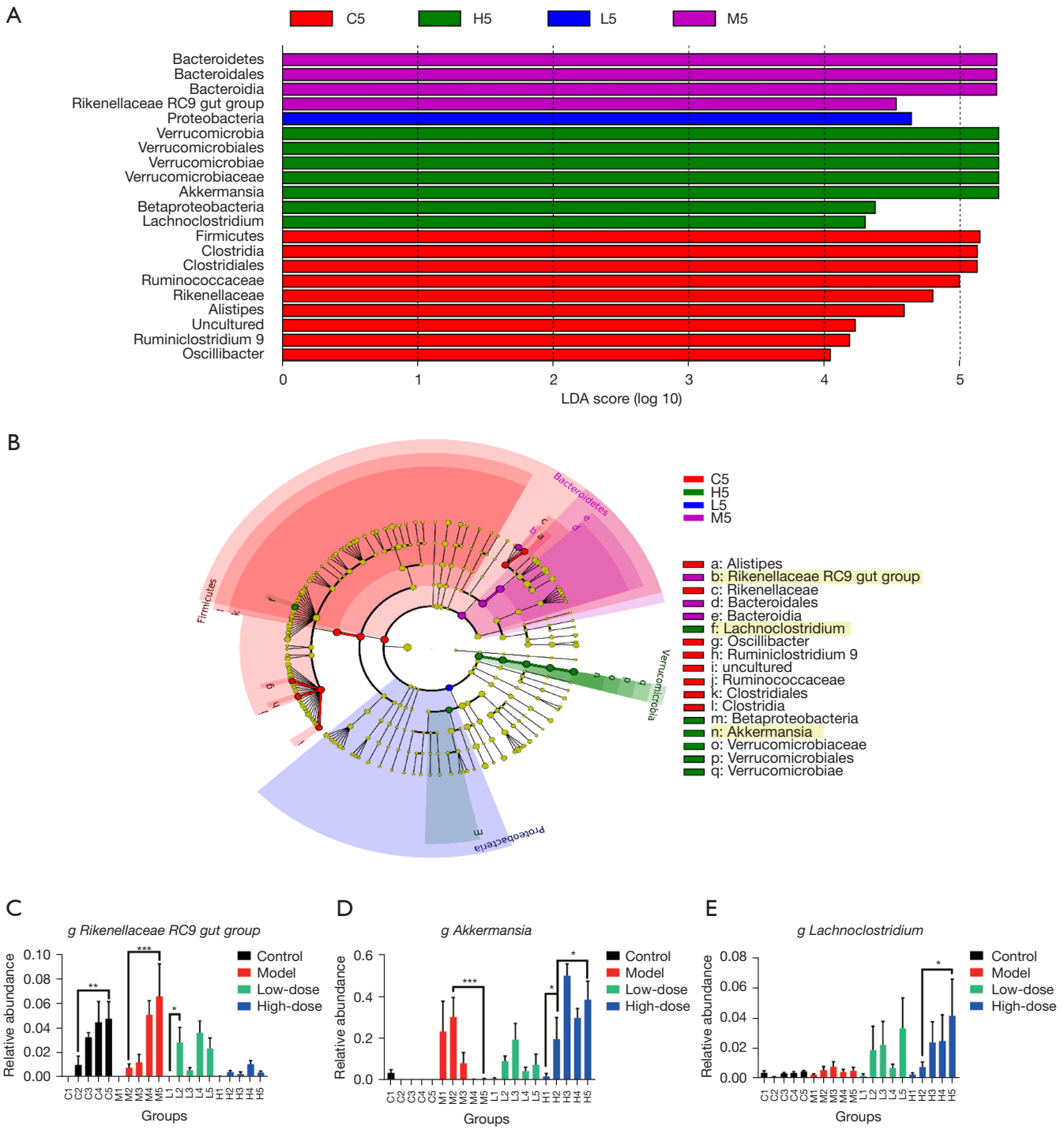

Figure 4 LEfSe analysis. (A) Bacteria observed between groups based on LDA scores >4; (B) cladogram based on LDA scores; (C) *Rikenellaceae_RC9_gut_group*; (D) *Akkermansia*; (E) *Lachnoclostridium*. *, P<0.05; **, P<0.01; ***, P<0.001. (n=5). LDA, linear discriminant analysis; LEfSe, linear discriminant analysis effect size.

© Annals of Translational Medicine. All rights reserved.

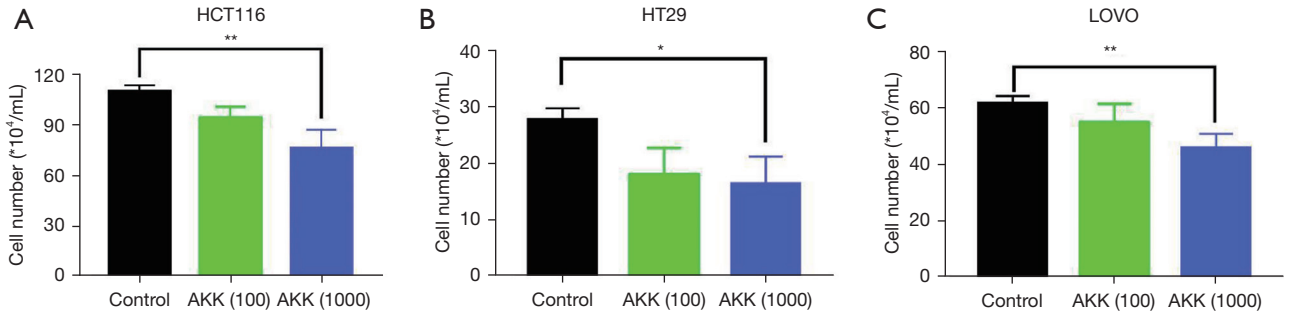

Figure 5 *Akkermansia* suppressed proliferation in CRC cells. (A) HCT-116, (B) HT-29, and (C) LOVO cells were exposed to *Akkermansia* (multiplicity of infection =100/1,000) for 4 hours. *, P<0.05; **, P<0.01. AKK, *Akkermansia muciniphila;* CRC, colorectal cancer.

play an important role in the anti-CRC effects of GC-K.

Acknowledgments

Funding: This work was supported by the National Natural Scientific Foundation of China (Nos. 82074000, 81903784); the Hunan Provincial Natural Science Foundation of China (No. 2020JJ4878); the Scientific Research Project of Department of Education of Hunan Province (No. 20K136); the Scientific Research Project of Hunan Administration of Traditional Chinese Medicine (No. 2021034); Postgraduate Scientific Research Innovation Project of Hunan Province (No. CX20200121); the Fundamental Research Funds for Central Universities of Central South University (No. 2020zzts252); and NHC Key Laboratory of Birth Defect for Research and Prevention (Hunan Provincial Maternal and Child Health Care Hospital, No. KF2020002).

Footnote

Reporting Checklist: The authors have completed the ARRIVE reporting checklist. Available at https://atm.amegroups.com/article/view/10.21037/atm-22-793/rc

Data Sharing Statement: Available at https://atm.amegroups.com/article/view/10.21037/atm-22-793/dss

Conflicts of Interest: All authors have completed the ICMJE uniform disclosure form (available at https://atm.amegroups.com/article/view/10.21037/atm-22-793/coif). The authors have no conflicts of interest to declare.

Ethical Statement: The authors are accountable for all aspects of the work in ensuring that questions related to the accuracy or integrity of any part of the work are appropriately investigated and resolved. The animal experimental protocol was approved by the Ethics Committee of Animal Experiments of Central South University (No. 201803070). Experiments were performed in compliance with the "Regulations on the Administration of Laboratory Animals" formulated by the National Science and Technology Commission of the People's Republic of China for the care and use of animals.

Open Access Statement: This is an Open Access article distributed in accordance with the Creative Commons Attribution-NonCommercial-NoDerivs 4.0 International License (CC BY-NC-ND 4.0), which permits the non-commercial replication and distribution of the article with the strict proviso that no changes or edits are made and the original work is properly cited (including links to both the formal publication through the relevant DOI and the license). See: https://creativecommons.org/licenses/by-nc-nd/4.0/.

References

1. Siegel RL, Miller KD, Fuchs HE, et al. Cancer Statistics, 2021. CA Cancer J Clin 2021;71:7-33.
2. Rogler G. Chronic ulcerative colitis and colorectal cancer. Cancer Lett 2014;345:235-41.
3. Rinninella E, Raoul P, Cintoni M, et al. What is the Healthy Gut Microbiota Composition? A Changing Ecosystem across Age, Environment, Diet, and Diseases. Microorganisms 2019;7:14.
4. Louis P, Hold GL, Flint HJ. The gut microbiota, bacterial metabolites and colorectal cancer. Nat Rev Microbiol 2014;12:661-72.
5. Brennan CA, Garrett WS. Gut Microbiota,

© Annals of Translational Medicine. All rights reserved.

Inflammation, and Colorectal Cancer. Annu Rev Microbiol 2016;70:395-411.
6. Wong SH, Yu J. Gut microbiota in colorectal cancer: mechanisms of action and clinical applications. Nat Rev Gastroenterol Hepatol 2019;16:690-704.
7. Gopalakrishnan V, Helmink BA, Spencer CN, et al. The Influence of the Gut Microbiome on Cancer, Immunity, and Cancer Immunotherapy. Cancer Cell 2018;33:570-80.
8. Rooks MG, Garrett WS. Gut microbiota, metabolites and host immunity. Nat Rev Immunol 2016;16:341-52.
9. Helmink BA, Khan MAW, Hermann A, et al. The microbiome, cancer, and cancer therapy. Nat Med 2019;25:377-88.
10. Guo YP, Shao L, Chen MY, et al. In Vivo Metabolic Profiles of Panax notoginseng Saponins Mediated by Gut Microbiota in Rats. J Agric Food Chem 2020;68:6835-44.
11. Guo YP, Chen MY, Shao L, et al. Quantification of Panax notoginseng saponins metabolites in rat plasma with in vivo gut microbiota-mediated biotransformation by HPLC-MS/MS. Chin J Nat Med 2019;17:231-40.
12. Chen MY, Shao L, Zhang W, et al. Metabolic analysis of Panax notoginseng saponins with gut microbiota-mediated biotransformation by HPLC-DAD-Q-TOF-MS/MS. J Pharm Biomed Anal 2018;150:199-207.
13. Yang XD, Yang YY, Ouyang DS, et al. A review of biotransformation and pharmacology of ginsenoside compound K. Fitoterapia 2015;100:208-20.
14. Oh J, Kim JS. Compound K derived from ginseng: neuroprotection and cognitive improvement. Food Funct 2016;7:4506-15.
15. Chen L, Meng Y, Sun Q, et al. Ginsenoside compound K sensitizes human colon cancer cells to TRAIL-induced apoptosis via autophagy-dependent and -independent DR5 upregulation. Cell Death Dis 2016;7:e2334.
16. Kim DY, Park MW, Yuan HD, et al. Compound K induces apoptosis via CAMK-IV/AMPK pathways in HT-29 colon cancer cells. J Agric Food Chem 2009;57:10573-8.
17. Zhang Z, Du GJ, Wang CZ, et al. Compound K, a Ginsenoside Metabolite, Inhibits Colon Cancer Growth via Multiple Pathways Including p53-p21 Interactions. Int J Mol Sci 2013;14:2980-95.
18. Paek IB, Moon Y, Kim J, et al. Pharmacokinetics of a ginseng saponin metabolite compound K in rats. Biopharm Drug Dispos 2006;27:39-45.
19. Chen L, Zhou L, Huang J, et al. Single- and Multiple-Dose Trials to Determine the Pharmacokinetics, Safety, Tolerability, and Sex Effect of Oral Ginsenoside Compound K in Healthy Chinese Volunteers. Front Pharmacol 2017;8:965.
20. Niu T, Smith DL, Yang Z, et al. Bioactivity and bioavailability of ginsenosides are dependent on the glycosidase activities of the A/J mouse intestinal microbiome defined by pyrosequencing. Pharm Res 2013;30:836-46.
21. Chen L, Chen MY, Shao L, et al. Panax notoginseng saponins prevent colitis-associated colorectal cancer development: the role of gut microbiota. Chin J Nat Med 2020;18:500-7.
22. Liu H, Yang J, Du F, et al. Absorption and disposition of ginsenosides after oral administration of Panax notoginseng extract to rats. Drug Metab Dispos 2009;37:2290-8.
23. Wang J, Shao L, Rao T, et al. Chemo-Preventive Potential of Falcarindiol-Enriched Fraction from Oplopanax elatus on Colorectal Cancer Interfered by Human Gut Microbiota. Am J Chin Med 2019;47:1381-404.
24. Jackson LN, Zhou Y, Qiu S, et al. Alternative medicine products as a novel treatment strategy for inflammatory bowel disease. Am J Chin Med 2008;36:953-65.
25. Naito S, von Eschenbach AC, Giavazzi R, et al. Growth and metastasis of tumor cells isolated from a human renal cell carcinoma implanted into different organs of nude mice. Cancer Res 1986;46:4109-15.
26. Hwang JA, Hwang MK, Jang Y, et al. 20-O- -d-glucopyranosyl-20(S)-protopanaxadiol, a metabolite of ginseng, inhibits colon cancer growth by targeting TRPC channel-mediated calcium influx. J Nutr Biochem 2013;24:1096-104.
27. Lu Y, Wang J, Ji Y, et al. Metabonomic Variation of Exopolysaccharide from Rhizopus nigricans on AOM/DSS-Induced Colorectal Cancer in Mice. Onco Targets Ther 2019;12:10023-33.
28. Chen J, Wu H, Wang Q, et al. Ginsenoside metabolite compound k alleviates adjuvant-induced arthritis by suppressing T cell activation. Inflammation 2014;37:1608-15.
29. Liu KK, Wang QT, Yang SM, et al. Ginsenoside compound K suppresses the abnormal activation of T lymphocytes in mice with collagen-induced arthritis. Acta Pharmacol Sin 2014;35:599-612.
30. Sun L, Jia H, Li J, et al. Cecal Gut Microbiota and Metabolites Might Contribute to the Severity of Acute Myocardial Ischemia by Impacting the Intestinal Permeability, Oxidative Stress, and Energy Metabolism. Front Microbiol 2019;10:1745.
31. Zhou L, Xiao X, Zhang Q, et al. Improved Glucose and

© Annals of Translational Medicine. All rights reserved.

Lipid Metabolism in the Early Life of Female Offspring by Maternal Dietary Genistein Is Associated With Alterations in the Gut Microbiota. Front Endocrinol (Lausanne) 2018;9:516.
32. Roopchand DE, Carmody RN, Kuhn P, et al. Dietary Polyphenols Promote Growth of the Gut Bacterium Akkermansia muciniphila and Attenuate High-Fat Diet-Induced Metabolic Syndrome. Diabetes 2015;64:2847-58.
33. Derrien M, Vaughan EE, Plugge CM, et al. Akkermansia muciniphila gen. nov., sp. nov., a human intestinal mucin-degrading bacterium. Int J Syst Evol Microbiol 2004;54:1469-76.
34. Zhang Z, Wu X, Cao S, et al. Chlorogenic Acid Ameliorates Experimental Colitis by Promoting Growth of Akkermansia in Mice. Nutrients 2017;9:677.
35. Zhai R, Xue X, Zhang L, et al. Strain-Specific Anti-inflammatory Properties of Two Akkermansia muciniphila Strains on Chronic Colitis in Mice. Front Cell Infect Microbiol 2019;9:239.
36. Wang L, Tang L, Feng Y, et al. A purified membrane protein from Akkermansia muciniphila or the pasteurised bacterium blunts colitis associated tumourigenesis by modulation of CD8+ T cells in mice. Gut 2020;69:1988-97.

(English Language Editor: C. Betlazar-Maseh)

Cite this article as: Shao L, Guo YP, Wang L, Chen MY, Zhang W, Deng S, Huang WH. Effects of ginsenoside compound K on colitis-associated colorectal cancer and gut microbiota profiles in mice. Ann Transl Med 2022;10(7):408. doi: 10.21037/atm-22-793

© Annals of Translational Medicine. All rights reserved.